arXiv:1402.3971v1 [hep-ph] 17 Feb 2014

The $\bar{K}N \to K\Xi$ reaction in coupled channel chiral models up to next-to-leading order

V.K. Magas[*,†], A. Feijoo[*] and A. Ramos[*,†]

[*]*Dept. d'Estructura i Constituents de la Matèria, Universitat de Barcelona, Martí Franquès 1, E08028 Barcelona, Spain*
[†]*Institut de Ciències del Cosmos, Universitat de Barcelona, Martí Franquès 1, E08028 Barcelona, Spain*

Abstract. We study the meson-baryon interaction in S-wave in the strangeness S=-1 sector using a chiral unitary approach based on a next-to-leading order chiral SU(3) Lagrangian. We fit our model to the large set of experimental data in different two-body channels. We pay particular attention to the $\bar{K}N \to K\Xi$ reaction, where the effect of the next-to-leading order terms in the Lagrangian are sufficiently large to be observed, since at tree level the cross section of this reaction is zero. For these channels we improve our approach by phenomenologically taking into account effects of the high spin hyperonic resonances.

Keywords: NLO chiral Lagrangian, Unitary extension of Chiral Perturbation Theory, Ξ production reactions, high spin resonances
PACS: 13.75.-n, 13.75.Jz, 12.39.Fe, 14.20.Jn

INTRODUCTION

In this work we aim to improve the chiral model description of the low energy hadron dynamics by taking into account effects of the next-to-leading (NLO) terms in the chiral Lagrangian. It is well known that Quantum Chromodynamics (QCD), the proper theory of strong interactions, is not applicable to study low energy hadron reactions. For such studies effective theories should be used, and SU(3) Chiral Perturbation Theory (χPT) is a classical example. This theory is based on an effective Lagrangian with hadron degrees of freedom, which respects the symmetries of QCD, in particular the chiral symmetry $SU(3)_R \times SU(3)_L$. In spite of the many successful applications of χPT, it fails to describe the hadron dynamics in the vicinity of dynamically generated resonances. A good example of such situation is the kaon-nucleon interaction at low momenta, where the perturbation scheme is violated by the presence of the $\Lambda(1405)$ resonance, located only 27 MeV below the $\bar{K}N$ threshold. In this case the use of some non-perturbative techniques is mandatory. In particular such a situation can be successfully studied within a unitary extension of Chiral Perturbation Theory (UχPT), originally proposed in [1], where the unitarization is implemented in coupled channels.

Interestingly, the $\Lambda(1405)$ resonance does not only give a reason to use UχPT theory, but also provides a good test of the predictive power of this approach. The point is that the $\Lambda(1405)$ is a dynamically generated resonance. This was predicted for the first time in 1977, see Ref. [2], and later detailed calculations performed in the framework of UχPT have shown that $\Lambda(1405)$ is actually a superposition of two close dynamically generated states. Most of such simulations [4, 5, 6, 7] predict one state at energy $\approx$ 1390 MeV with larger width $\approx$ 130 MeV, which couples most strongly to $\Sigma\pi$ channels; and the other one at higher energy $\approx$ 1420 MeV and with a much narrower width $\approx$ 30 MeV, which couples most strongly to $\bar{K}N$ channels. [1] Thus, the experimental shape of the $\Lambda(1405)$ resonance depends on the details of the given experiment, namely on the relative weight of the $\Sigma\pi$ and $\bar{K}N$ channels in the given reaction. This rather nontrivial prediction has been finally confirmed experimentally, see Ref. [3] for more details.

[1] Although a recent study [8] predicts rather different positions for the two $\Lambda(1405)$ state. This work is also interesting in connection with our study because the authors perform calculations based on NLO Chiral Lagrangian, but they do not take into consideration the η and Ξ channels (their effects are "included" by renormalizing other model parameters), while for us the latter ones are of crucial importance.

FORMALISM

In this section, we briefly outline the coupled-channel formalism of meson-baryon scattering. It is based on the SU(3) chiral effective Lagrangian which incorporates the same symmetries and symmetry breaking patterns as QCD and describes the coupling of the pseudoscalar octet (π, K, η) to the ground state baryon octet $(N, \Lambda, \Sigma, \Xi)$. The Lagrangian

$$\mathscr{L} = \mathscr{L}_\phi + \mathscr{L}_{\phi B} \tag{1}$$

includes the mesonic term $\mathscr{L}_\phi$ up to second chiral order [14],

$$\mathscr{L}_\phi = \frac{f^2}{4}\langle u_\mu u^\mu \rangle + \frac{f^2}{4}\langle \chi_+ \rangle, \tag{2}$$

where $\langle \ldots \rangle$ denotes the trace in flavor space. The pseudoscalar meson octet ϕ is arranged in a matrix valued field

$$U(\phi) = u^2(\phi) = \exp\left(\sqrt{2}i\frac{\phi}{f}\right) \tag{3}$$

and f is the pseudoscalar decay constant in the chiral limit. The quantity U enters the Lagrangian in the combinations $u_\mu = iu^\dagger \partial_\mu U u^\dagger$ and $\chi_+ = 2B_0(u^\dagger \mathscr{M} u^\dagger + u \mathscr{M} u)$, the latter one involving explicit chiral symmetry breaking via the quark mass matrix $\mathscr{M} = \mathrm{diag}\,(m_u, m_d, m_s)$, and $B_0 = -\langle 0|\bar{q}q|0\rangle / f^2$ relates to the order parameter of spontaneously broken chiral symmetry.

The second piece of the Lagrangian in eq. (1), $\mathscr{L}_{\phi B}$, describes the meson-baryon interactions and reads at lowest order [15]

$$\mathscr{L}^{(1)}_{\phi B} = i\langle \bar{B}\gamma_\mu [D^\mu, B]\rangle - M_0\langle \bar{B}B\rangle - \frac{1}{2}D\langle \bar{B}\gamma_\mu\gamma_5\{u^\mu, B\}\rangle - \frac{1}{2}F\langle \bar{B}\gamma_\mu\gamma_5[u^\mu, B]\rangle. \tag{4}$$

The 3×3 matrix B collects the ground state baryon octet, M_0 is the common baryon octet mass in the chiral limit and D, F denote the axial vector couplings of the baryons to the mesons. Their numerical values can be extracted from semileptonic hyperon decays and we employ the central values determined in [16]: $D = 0.80$, $F = 0.46$. The covariant derivative of the baryon field is given by

$$[D_\mu, B] = \partial_\mu B + [\Gamma_\mu, B] \tag{5}$$

with the chiral connection

$$\Gamma_\mu = \tfrac{1}{2}[u^\dagger, \partial_\mu u]. \tag{6}$$

We also need the next-to-leading order contribution to $\mathscr{L}_{\phi B}$ which is given by

$$\begin{aligned}\mathscr{L}^{(2)}_{\phi B} \;=\;& b_D\langle \bar{B}\{\chi_+, B\}\rangle + b_F\langle \bar{B}[\chi_+, B]\rangle + b_0\langle \bar{B}B\rangle\langle \chi_+\rangle \\ &+ d_1\langle \bar{B}\{u_\mu, [u^\mu, B]\}\rangle + d_2\langle \bar{B}[u_\mu, [u^\mu, B]]\rangle + d_3\langle \bar{B}u_\mu\rangle\langle u^\mu B\rangle + d_4\langle \bar{B}B\rangle\langle u^\mu u_\mu\rangle,\end{aligned} \tag{7}$$

where only the pieces relevant for our analysis are displayed.

Then the interaction kernel for (i, j) channels, V_{ij}, can be calculated from the chiral Lagrangian up to the corresponding order in momentum over baryon mass. For the meson-baryon interaction, the lowest order term in momentum, i.e. leading order (LO) term, is the so called Weimberg-Tomozawa (WT) term:

$$V^{WT}_{ij} = -C_{ij}\frac{1}{4f^2}\bar{u}^{s'}_{B'}(p')\gamma^\mu u^s_B(p)(k_\mu + k'_\mu)\,, \tag{8}$$

which depends only on one parameter - the pion decay constant f. C_{ij} is a matrix of coefficients; k^μ and k'^μ are the four-momenta for the incoming and outgoing mesons in the process; $u^s_B(p)$ is the incoming baryon with s spin and p momentum, and analogously for the $\bar{u}^{s'}_{B'}(p')$ of the outgoing baryon. The pion decay constant is well known experimentally, $f_{exp} = 93.4\ MeV$, however in LO UχPT calculations this parameters is usually taken to be $f = 1.15 - 1.2\, f_{exp}$, in order to partly simulate the effect of the higher order corrections.

The interaction kernel up to NLO is also known:

$$V^{NLO}_{ij} = V^{WT}_{ij} + \frac{1}{f^2}\bar{u}^{s'}_{B'}(p')\left(D_{ij} - 2(k_\mu k'^\mu)L_{ij}\right)u^s_B(p)\sqrt{\frac{M_i + E_i}{2M_i}}\sqrt{\frac{M_j + E_j}{2M_j}} \tag{9}$$

where D_{ij} and L_{ij} are the coefficient matrixes, which depend on the new parameters: b_0, b_D, b_F, d_1, d_2, d_3, d_4 (see [5, 6, 7, 10, 11, 12] for more details). However only very recently it has started to be used in real calculations and data fitting [5, 6, 7, 8, 10, 11, 12, 13]. The reason is rather straightforward - NLO terms in the chiral Lagrangian depend on 7 new parameters, which were not known, and thus the predictive power of the NLO UχPT calculations was rather questionable.

Thanks to great experimental advances of the last years, like for example CLAS photoproduction experiments [17], we have accumulated a sufficient amount of a good quality data to attempt to fit these new parameters. Also due to the large amount of theoretical studies based on the WT interaction we know where this approach fails to describe the data. In particular, in our study we concentrate on the Ξ hyperon production reactions: $K^- p \to K^+\Xi^-, K^0\Xi^0$, where the effect of the NLO terms in the Lagrangian play a crucial role, since the cross sections are zero at tree level of the WT term. These reactions are also particularly interesting, because they were not considered in the works of the other groups [5, 6, 7, 8, 10, 11].

The UχPT method consists in solving the Lippmann-Schwinger (LS) equations in coupled channels, which is reduced to a system of algebraic equations [9]:

$$T_{ij} = V_{ij} + V_{il} G_l T_{lj}\,, \tag{10}$$

where T_{ij} is the scattering amplitude for the transition from channel "i" to channel "j"; the subscripts run over all the possible channels. In particular, for the meson-baryon interaction in the $S=-1$ sector, which is of prime interest for us, there are the following 10 channels: $K^- p$, $\bar{K}^0 n$, $\pi^0\Lambda$, $\pi^0\Sigma^0$, $\pi^+\Sigma^-$, $\pi^-\Sigma^+$, $\eta\Lambda$, $\eta\Sigma^0$, $K^+\Xi^-$, $K^0\Xi^0$.

In our study we calculate the loop function, G_l, using a dimensional regularization scheme:

$$G_l = \frac{2M_l}{(4\pi)^2}\left\{a_l + \ln\frac{M_l^2}{\mu^2} + \frac{m_l^2 - M_l^2 + s}{2s}\ln\frac{m_l^2}{M_l^2} + \frac{q_{cm}}{\sqrt{s}}\ln\left[\frac{(s+2\sqrt{s}q_{cm})^2 - (M_l^2 - m_l^2)^2}{(s-2\sqrt{s}q_{cm})^2 - (M_l^2 - m_l^2)^2}\right]\right\}, \tag{11}$$

where M_l and m_l are the baryon and meson masses of the "l" channel correspondingly, and a_l are the so called subtraction constants, which are used as free parameters and fitted to the experimental data. Taking into account the isospin symmetry there are only 6 independent subtraction constants. See Ref. [9] for more details.

Having calculated the T-matrix by solving the system of equations (10), $T^{LS}(s',s)$, we can obtain the unpolarized cross-section for the $i \to j$ reaction in the usual way:

$$\frac{d\sigma_{ij}}{d\Omega} = \frac{1}{64\pi^2}\frac{4M_iM_j}{s}\frac{k_j}{k_i}M_{ij}\,; \quad M_{ij} = \frac{1}{2}\sum_{s',s}|T_{ij}^{LS}(s',s)|^2 \tag{12}$$

Inclusion of heavy high spin hyperonic resonances in $\bar{K}N \to K\Xi$ transitions

However, our previous studies [12, 13], together with the phenomenological work [29], indicate the necessity to take into consideration the $\bar{K}N \to Y \to K\Xi$ reactions, where Y stands for some high spin resonance, which couples to these channels. A lot of Y resonances are known in the relevant energy range. The PDG compilation [32] gives eight resonances of four- and three-star status with $1.89 < M < 2.35$ GeV, see table 1. On the other hand, branching ratios of $K\Xi$ decay are determined for none of them. Only for two of them, upper limits [3% for $\Lambda(2100)$ and 2% for $\Sigma(2030)$] are deduced [32].

Naturally, the main decay channels for all these resonances are $\pi\Lambda$ (for Σ resonances), $\pi\Sigma$, and $\overline{K}N$, while the branching ratios of $K\Xi$ decay are small, since the $K\Xi$ decay requires creation of an additional $\bar{s}s$ pair and it is not so favorable energetically. On the other hand, cross sections of the $\overline{K}N \to K\Xi$ reaction are more than two orders of magnitude smaller than, for example $\overline{K}N \to \pi\Sigma$ and $\overline{K}N \to \overline{K}N$, so even small branching ratios can contribute sizably to the former reaction. Thus, the role of the above-threshold resonances should be studied. Most of these resonances have high spins, and therefore require a special treatment, analogous to that performed in [29, 30, 31].

Based on our fit presented in [13] it seems that the $\Sigma(2030)$ and the $\Sigma(2250)$ resonances would be good candidates to be considered, and this observation coincides with the finding of [29]. Spin and parity ($J^\pi = 7/2^+$) of the $\Sigma(2030)$ are well established. For the $\Sigma(2250)$, most probable assignments are $5/2^-$ and $9/2^-$ [32]. We choose $J^\pi = 5/2^-$ to simplify the calculations.[2] We fix the masses of the resonances to their nominal values, 2030 MeV and 2250 MeV, and

[2] It has also been shown in [29] that the $9/2^-$ choice do not change the results drastically.

TABLE 1. Hyperonic four- and three-star resonances in the range $1.89 < M < 2.35$ GeV listed in PDG [32].

Resonance	$I\,(J^P)$	**Mass** (MeV)	$\Gamma\,(MeV)$	$\Gamma_{K\Xi}/\Gamma$
$\Lambda(1890)$	$0\left(\frac{3}{2}^+\right)$	1850 - 1910	60 - 200	
$\Lambda(2100)$	$0\left(\frac{7}{2}^-\right)$	2090 - 2110	100 - 250	$< 3\%$
$\Lambda(2110)$	$0\left(\frac{5}{2}^+\right)$	2090 - 2140	150 - 250	
$\Lambda(2350)$	$0\left(\frac{9}{2}^+\right)$	2340 - 2370	100 - 250	
$\Sigma(1915)$	$1\left(\frac{5}{2}^+\right)$	1900 - 1935	80 - 160	
$\Sigma(1940)$	$1\left(\frac{3}{2}^-\right)$	1900 - 1950	150 - 300	
$\Sigma(2030)$	$1\left(\frac{7}{2}^+\right)$	2025 - 2040	150 - 200	$< 2\%$
$\Sigma(2250)$	$1\left(?^?\right)$	2210 - 2280	60 - 150	

their widths to 175 MeV and 105 MeV respectively. The latter quantities are the median values of the ranges presented for the widths in the PDG compilation [32].

Thus, in order to calculate the $\overline{K}N \to K^+\Xi^-$, $K^0\Xi^0$ reaction cross sections we add to the corresponding $T^{LS}(s',s)$ amplitude the contributions from the $\overline{K}N \to \Sigma(2030) \to K\Xi$ and $\overline{K}N \to \Sigma(2250) \to K\Xi$ scattering amplitudes, which we denote by $T^{7/2^+}(s',s)$ and $T^{5/2^-}(s',s)$ correspondingly.

As in [31], we adopt the Rarita-Schwinger method to describe spin-5/2 and 7/2 baryon fields, which are given as a rank-2 tensor $Y^{\mu\nu}_{5/2}$ and as a rank-3 tensor $Y^{\mu\nu\alpha}_{7/2}$ respectively.

$$\mathscr{L}^{5/2^\pm}_{BYK}(q) = i\frac{g_{BY_{5/2}K}}{m_K^2}\bar{B}\Gamma^{(\pm)}Y^{\mu\nu}_{5/2}\partial_\mu\partial_\nu K + H.c.\,, \quad \mathscr{L}^{7/2^\pm}_{BYK}(q) = -\frac{g_{BY_{7/2}K}}{m_K^3}\bar{B}\Gamma^{(\mp)}Y^{\mu\nu\alpha}_{7/2}\partial_\mu\partial_\nu\partial_\alpha K + H.c.\,, \tag{13}$$

where $\Gamma^{(\pm)} = \binom{\gamma_5}{1}$. Then the corresponding propagators are given by [31]:

$$S_{5/2}(q) = \frac{i}{\not{q} - M_{Y_{5/2}} + i\Gamma_{5/2}/2}\Delta^{\beta_1\beta_2}_{\alpha_1\alpha_2}\,, \quad S_{7/2}(q) = \frac{i}{\not{q} - M_{Y_{7/2}} + i\Gamma_{7/2}/2}\Delta^{\beta_1\beta_2\beta_3}_{\alpha_1\alpha_2\alpha_3}\,, \tag{14}$$

where we have included the decay width, Γ_J, of the corresponding resonance, and tensors Δ are defined as follows:

$$\Delta^{\beta_1\beta_2}_{\alpha_1\alpha_2}\left(\frac{5}{2}\right) = \frac{1}{2}\left(\theta^{\beta_1}_{\alpha_1}\theta^{\beta_2}_{\alpha_2} + \theta^{\beta_2}_{\alpha_1}\theta^{\beta_1}_{\alpha_2}\right) - \frac{1}{2}\theta_{\alpha_1\alpha_2}\theta^{\beta_1\beta_2} - \frac{1}{10}\left(\bar{\gamma}_{\alpha_1}\bar{\gamma}^{\beta_1}\theta^{\beta_2}_{\alpha_2} + \bar{\gamma}_{\alpha_1}\bar{\gamma}^{\beta_2}\theta^{\beta_1}_{\alpha_2} + \bar{\gamma}_{\alpha_2}\bar{\gamma}^{\beta_1}\theta^{\beta_2}_{\alpha_1} + \bar{\gamma}_{\alpha_2}\bar{\gamma}^{\beta_2}\theta^{\beta_1}_{\alpha_1}\right), \tag{15}$$

$$\Delta^{\beta_1\beta_2\beta_3}_{\alpha_1\alpha_2\alpha_3}\left(\frac{7}{2}\right) = \frac{1}{36}\sum_{P(\alpha)P(\beta)}\left(\theta^{\beta_1}_{\alpha_1}\theta^{\beta_2}_{\alpha_2}\theta^{\beta_3}_{\alpha_3} - \frac{3}{7}\theta^{\beta_1}_{\alpha_1}\theta_{\alpha_2\alpha_3}\theta^{\beta_2\beta_3} - \frac{3}{7}\bar{\gamma}_{\alpha_1}\bar{\gamma}^{\beta_1}\theta^{\beta_2}_{\alpha_2}\theta^{\beta_3}_{\alpha_3} + \frac{3}{35}\bar{\gamma}_{\alpha_1}\bar{\gamma}^{\beta_1}\theta_{\alpha_2\alpha_3}\theta^{\beta_2\beta_3}\right), \tag{16}$$

where $\theta^\nu_\mu = g^\nu_\mu - \frac{q_\mu q^\nu}{M_Y^2}$, $\bar{\gamma}_\mu = \gamma_\mu - \frac{q_\mu \not{q}}{M_Y^2}$ with M_Y being the pertinent resonance mass. In eq. (16) the tensor for the spin-7/2 field contains summation over all possible permutations of Dirac indexes $\{\alpha_1\alpha_2\alpha_3\}$ and $\{\beta_1\beta_2\beta_3\}$.

From the Lagrangians of eq. (13) one derives the baryon-kaon-Y_J vertices:

$$v^{5/2^\pm}_{BYK} = i\frac{g_{BY_{5/2}K}}{m_K^2}k_\mu k_\nu\Gamma^{(\pm)}\,, \quad v^{7/2^\pm}_{BYK} = -\frac{g_{BY_{7/2}K}}{m_K^3}k_\mu k_\nu k_\sigma\Gamma^{(\mp)}\,, \tag{17}$$

and the scattering amplitude for $\overline{K}N \to K\Xi$ reaction can be obtained straightforwardly:

$$T^{5/2^-}(s',s) = \frac{g_{\Xi Y_{5/2}K}g_{NY_{5/2}\overline{K}}}{m_K^4}\bar{u}^{s'}_\Xi(p')\frac{k'_{\beta_1}k'_{\beta_2}\Delta^{\beta_1\beta_2}_{\alpha_1\alpha_2}k^{\alpha_1}k^{\alpha_2}}{\not{q} - M_{Y_{5/2}} + i\Gamma_{5/2}/2}u^s_N(p)\exp\left(-\vec{k}^2/\Lambda^2_{5/2}\right)\exp\left(-\vec{k'}^2/\Lambda^2_{5/2}\right), \tag{18}$$

$$T^{7/2^+}(s',s) = \frac{g_{\Xi Y_{7/2}K}g_{NY_{7/2}\overline{K}}}{m_K^6}\bar{u}^{s'}_\Xi(p')\frac{k'_{\beta_1}k'_{\beta_2}k'_{\beta_2}\Delta^{\beta_1\beta_2\beta_3}_{\alpha_1\alpha_2\alpha_3}k^{\alpha_1}k^{\alpha_2}k^{\alpha_3}}{\not{q} - M_{Y_{7/2}} + i\Gamma_{7/2}/2}u^s_N(p)\exp\left(-\vec{k}^2/\Lambda^2_{7/2}\right)\exp\left(-\vec{k'}^2/\Lambda^2_{7/2}\right), \tag{19}$$

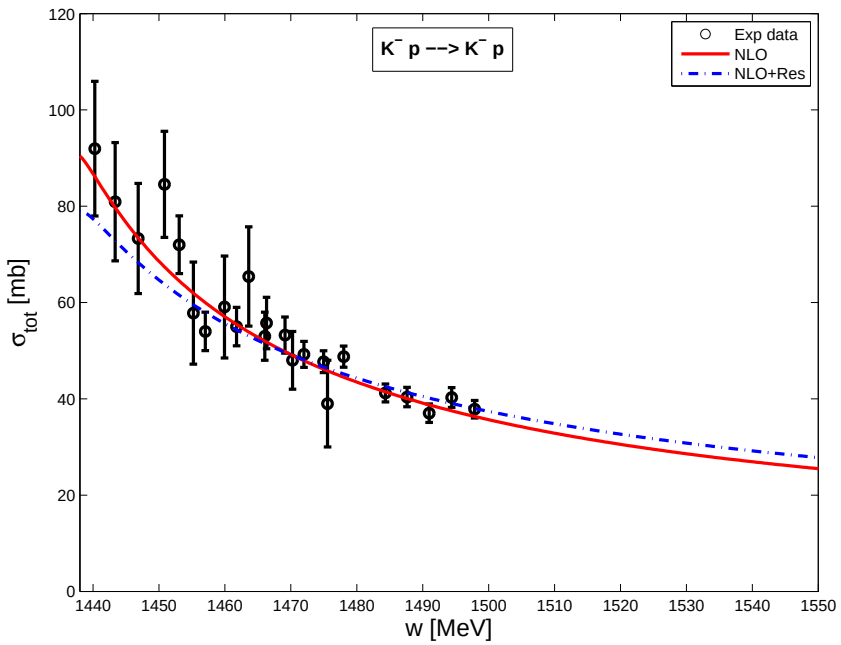

FIGURE 1. The total cross section of the $K^- p \to K^- p$ reaction. The solid line represents results of NLO fit, the dashed-dotted line - NLO+Res fit, see text for more details. Experimental data are from [22, 23, 24, 25, 26, 27, 28].

TABLE 2. This table shows the branching ratios at threshold for the NLO and NLO+Res fits, presented in Table 3, and the corresponding experimental values.

	γ	R_n	R_c
NLO	2.36	0.197	0.659
NLO+RES	2.37	0.193	0.657
Exp.	2.36 ± 0.04	0.189 ± 0.015	0.664 ± 0.011

where we have introduced phenomenological form factors, $\exp\left(-\vec{q}^{\,2}/\Lambda_j^2\right)$, associated with each vertex, in order to suppress high momentum contributions, as it was also done in [29].

Finally, for the initial channels $i = K^- p$, $\overline{K}^0 n$ and final channels $j = K^+\Xi^-$, $K^0\Xi^0$ we obtain

$$T_{ij}^{tot}(s',s) = \sqrt{4M_p M_\Xi}\, T_{ij}^{LS}(s',s) + T^{5/2^-}(s',s) + T^{7/2^+}(s',s)\,. \tag{20}$$

And then we can proceed following Eqs. (12).

RESULTS AND CONCLUSIONS

We will fit the available experimental data on cross sections for the transitions from the $K^- p$ initial state to different final states, some examples are presented in Figs. 1-4, as well as the threshold branching ratios:

$$\gamma = \frac{\Gamma(K^- p \to \pi^+\Sigma^-)}{\Gamma(K^- p \to \pi^-\Sigma^+)},\; R_n = \frac{\Gamma(K^- p \to \pi^0\Lambda)}{\Gamma(K^- p \to neutral\,states)},\; R_c = \frac{\Gamma(K^- p \to \pi^+\Sigma^-, \pi^-\Sigma^+)}{\Gamma(K^- p \to inelastic\,channels)},$$

given in Table 2.

We perform 14 and 17 parameter fits:

1) NLO interaction kernel without additional resonance contributions (NLO fit), 14 free parameters: the pion decay

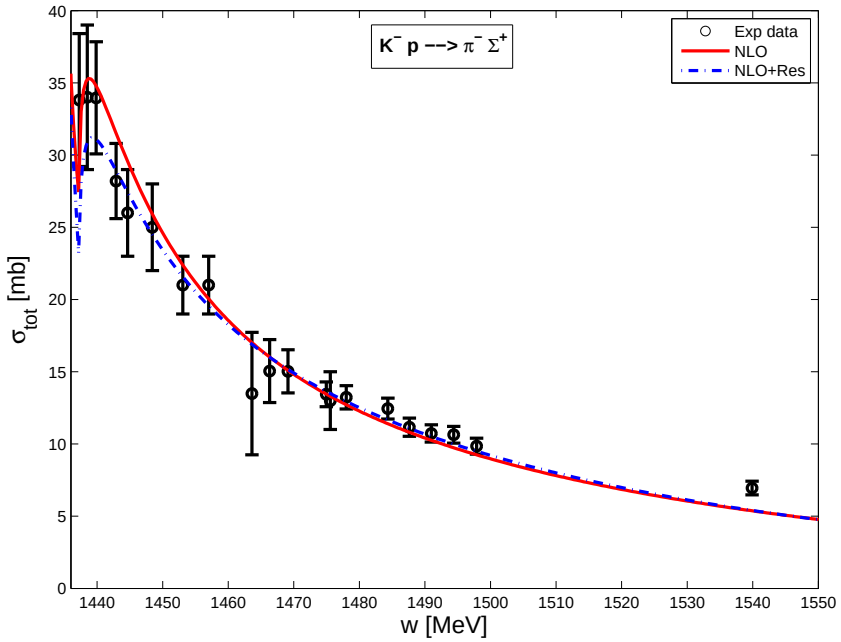

FIGURE 2. The total cross section of the $K^- p \to \pi^- \Sigma^+$ reaction. The solid line represents results of NLO fit, the dashed-dotted line - NLO+Res fit, see text for more details. Experimental data are from [22, 23, 24, 25, 26, 27, 28].

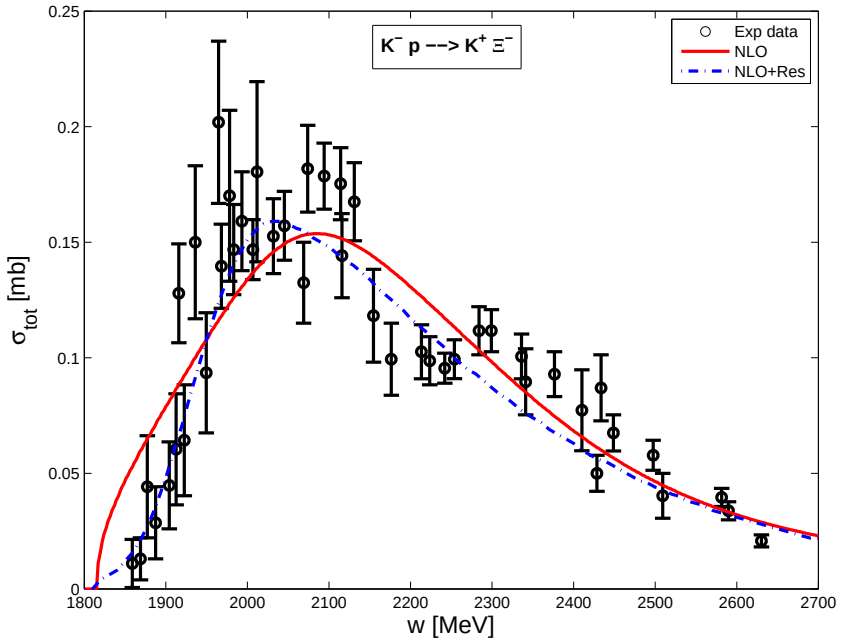

FIGURE 3. The total cross section of the $K^- p \to K^+ \Xi^-$ reaction. The solid line represents results of NLO fit, the dashed-dotted line - NLO+Res fit, see text for more details. Experimental data are from [22, 23, 24, 25, 26, 27, 28].

constant, 6 subtraction constants, and 7 NLO parameters (b_0, b_D, b_F, d_1, d_2, d_3, d_4);
2) NLO interaction kernel with high spin resonance contributions in $K^- p \to K^+ \Xi^-$, $K^0 \Xi^0$ channels (NLO+Res fit), 17 free parameters: 14 are the same as above, the new parameters are: effective couplings of the $Y_{5/2}$ and $Y_{7/2}$ resonances, and Λ_J parameter which defines the form factors of the resonances (as a first approximation we choose $\Lambda_{5/2} = \Lambda_{7/2}$).

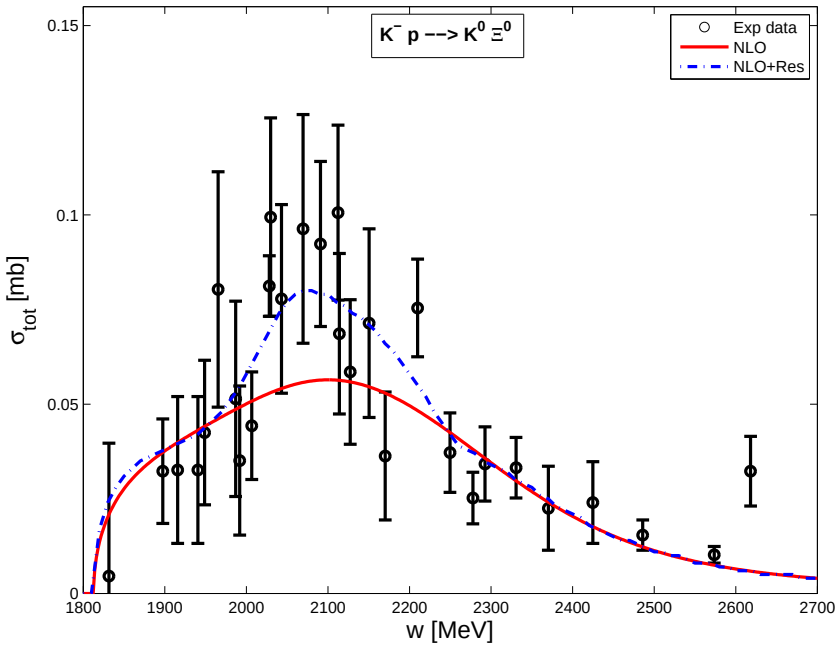

FIGURE 4. The total cross section of the $K^- p \to K^0 \Xi^0$ reaction. The solid line represents results of NLO fit, the dashed-dotted line - NLO+Res fit, see text for more details. Experimental data are from [22, 23, 24, 25, 26, 27, 28].

TABLE 3. Results of the NLO (14 parameters) and NLO+Res (17 parameters) fits, see text for more details.

	NLO	**NLO+RES**
$a_{\overline{K}N}$ (10^{-3})	4.64	6.84
$a_{\pi\Lambda}$ (10^{-3})	24.52	28.75
$a_{\pi\Sigma}$ (10^{-3})	2.06	0.79
$a_{\eta\Lambda}$ (10^{-3})	-9.10	-11.53
$a_{\eta\Sigma}$ (10^{-3})	-8.43	-13.53
$a_{K\Xi}$ (10^{-3})	37.54	29.71
f	$1.19 f_\pi$	$1.18 f_\pi$
b_0 (GeV^{-1})	-0.37	-0.31
b_D (GeV^{-1})	-0.04	- 0.11
b_F (GeV^{-1})	0.37	0.26
d_1 (GeV^{-1})	0.24	0.14
d_2 (GeV^{-1})	0.41	0.42
d_3 (GeV^{-1})	0.74	0.74
d_4 (GeV^{-1})	-0.58	-0.60
$g_{\Xi Y_{5/2} K} \cdot g_{N Y_{5/2} \overline{K}}$	-	84.12
$g_{\Xi Y_{7/2} K} \cdot g_{N Y_{7/2} \overline{K}}$	-	283.47
$\Lambda_{5/2} = \Lambda_{7/2}$ (MeV)	-	308.13
$\chi^2/d.o.f.$	1.88	1.40

The obtained parameter values and resulting $\chi^2/d.o.f.$ are presented in Table 3.

First of all, we would like to stress that the inclusion of the NLO terms into the interaction kernel substantially improves the agreement with data with respect to WT fits. This has been shown in detail in Refs. [10, 6, 11, 12, 7], and we are not going to discuss these aspects in the present letter.

Looking at Figs. 1, 2 and Tables 2, 3 we can conclude that for the observables unrelated to the Ξ hyperon production

reactions the model is only slightly modified, although the agreement with data is a little bit better. While on Figs. 3, 4 we see a substantial improvement in describing the $\bar{K}N \to K\Xi$ transitions, which are the key point of this work, as well as of the previous study [12, 13]. The improvement in these two channels is the main reason of the $\chi^2/d.o.f.$ reduction from NLO fit to NLO+Res one, see Table 3.

As it was discussed above these channels are extremely sensitive to the NLO corrections and therefore may play a crucial role in determining the NLO parameters. Comparing the NLO and NLO+Res fits in Table 3 we can see that the most drastic change has to do with the b_D parameter, the other sensitive ones are b_F, d_1, and b_0.

The final goal of our study is to find trustable restrictions on the 7 NLO parameters of the chiral Lagrangian. We would like to stress that, technically, to change in the calculations the WT interaction, eq. (8), to the NLO interaction, eq. (9), is rather straightforward. The problem comes from the fact that the 7 new parameters of the NLO interaction are not well controlled at the moment. Once stable values for these parameters are obtained, all the groups doing simulations based on the chiral Lagrangian will be able to increase the accuracy of their calculations to the next order with a rather little effort. Based on the presented results we believe that the inclusion of high spin hyperonic resonances in $K^- p \to K^+\Xi^-$, $K^0\Xi^0$ channels (which are 0 at three level in LO) is mandatory in order to obtain reliable NLO parameters.

ACKNOWLEDGMENTS

This work is supported by the European Community - Research Infrastructure Integrating Activity Study of Strongly Interacting Matter (HadronPhysics3, Grant Agreement Nr 283286) under the 7th Framework Programme, by the contract FIS2011-24154 from MICINN (Spain), and by the Generalitat de Catalunya, contract 2009SGR-1289.

REFERENCES

1. N. Kaiser, P. B. Siegel, W. Weise, Nucl. Phys. A **594**, 325 (1995).
2. M. Jones, R. H. Dalitz and R. R. Horgan, Nucl. Phys. B **129**, 45 (1977).
3. V.K. Magas, E. Oset, A. Ramos, Phys. Rev. Lett. **95**, 052301 (2005).
4. D. Jido, J. A. Oller, E. Oset, A. Ramos and U. G. Meissner, Nucl. Phys. A **725**, 181 (2003);
5. B. Borasoy, U. -G. Meissner and R. Nissler, Phys. Rev. C **74**, 055201 (2006).
6. Y. Ikeda, T. Hyodo, W. Wiese, Nucl. Phys. A **881**, 98 (2012).
7. Zhi-Hui Guo, J. A. Oller, Phys. Rev. C **87**, 035202 (2013).
8. M. Mai and U. -G. Meissner, Nucl. Phys. A **900**, 51 (2013).
9. E. Oset, A. Ramos, Nucl. Phys. A **636**, 99 (1998).
10. B. Borasoy, R. Niβler, W. Wiese, Eur. Phys. J. A **25**, 79 (2005).
11. T. Hyodo, D. Jido, Progress in Particle and Nuclear Physics **67**, 55 (2012).
12. A. Feijoo, Master Thesis (Master Interuniversitario de Fisica Nuclear), Universidad de Barcelona, Spain, 2012.
13. V. K. Magas, A. Feijoo and A. Ramos, arXiv:1311.5025 [hep-ph].
14. J. Gasser and H. Leutwyler, Nucl. Phys. **B250** (1985) 465.
15. A. Krause, Helv. Phys. Acta **63** (1990) 3.
16. F. E. Close and R. G. Roberts, Phys. Lett. **B316** (1993) 165;
    B. Borasoy, Phys. Rev. **D 59** (1999) 054021.
17. K. Moriya *et al.* [CLAS Collaboration], Phys. Rev. C **87**, 035206 (2013).
18. R. O. Bangerter, et al., Phys. Rev. D **23**, 1484 (1981).
19. J. Ciborowski, et al., J. Phys. G **8**, 13 (1982).
20. T. S. Mast, et al., Phys. Rev. D **14**, 13 (1976).
21. J. K. Kim, Phys. Rev. Lett. **14**, 89 (1965).
22. G. Burgun et al., Nucl. Phys. B **8**, 447 (1968).
23. J. R. Carlson, et al., Phys. Rev. D **7**, 2533 (1973).
24. P. M. Dauber, et al., Phys. Rev. **179**, 1262 (1969).
25. M. Haque et al., Phys. Rev. **152**, 1148 (1966).
26. G. W. London, et al., Phys. Rev. **143**, 1034 (1966).
27. T. G. Trippe, P. E. Schlein, Phys. Rev. **158**, 1334 (1967).
28. W. P. Trower, et al., Phys. Rev. **170**, 1207 (1968).
29. D. A. Sharov, V. L. Korotkikh, D. E. Lanskoy, Eur. Phys. J. A **47**, 109 (2011).
30. K. Nakayama, Y. Oh and H. Habertzettl, Phys. Rev. C **74**, 035205 (2006).
31. K. Shing Man, Y. Oh and K. Nakayama,, Phys. Rev. C **83**, 055201 (2011).
32. J. Beringer *et al.*, (Particle Data Group), Phys. Rev. D **86**, 010001 (2012).